Experimental research on spatial filtering of deformed laser beam by transmitting volume Bragg grating

Guangwei Zheng (郑光威)[1,2*], Benjian Shen (沈本剑)[3], Jichun Tan (谭吉春)[3], Yanlan He (何焰蓝)[3], and Xiao Wang (王 逍)[4]

[1] *College of Optoelectronic science and engineering, National University of Defense Technology, Changsha 410073, China*

[2] *Telecommunication Engineering Institute, Air Force Engineering University, Xi'an 710077, China*

[3] *College of science, National University of Defense Technology, Changsha 410073, China*

[4] *Research Center of Laser Fusion, Chinese Academy of Engineering Physics, Mianyang 621900, China*

[*] *Corresponding author: zgw198196@126.com*

Received August 24, 2010; accepted November 19, 2010; posted online February 21,2011

Using transmitting volume Bragg gratings (TVBG) as a basis, an experiment on one-dimensional spatial filtering of a deformed laser beam is designed. The deformed laser beam results from a He-Ne laser beam modulated by an amplitude modulation plate with a spatial frequency of 7.2 mm^{-1}. Results show that when the central wave vector of the deformed beam satisfies the Bragg law of TVBG, the spatial profile of the −1st forward-diffracted order is similar to that of the undeformed He-Ne laser beam due to the TVBG with a spatial frequency selective bandwidth of less than 5.0 mm^{-1}. The higher frequency components of the deformed beam are filtered out in the optical near field. Thus, the TVBG cleanup of the spatially-deformed laser beam is realized experimentally.

OCIS codes: 050.1940, 050.7330, 070.6110, 090.1970.

doi: 10.3788/COL201109.030501.

Because of high diffraction efficiency and excellent wave vector selectivity, transmitting volume Bragg gratings (TVBG) have been extensively applied in numerous optical systems, such as coherent or incoherent beam combinations, spatial filtering of laser beams, temporal shaping of laser pulses, beam quality optimization of diode lasers, and so on[1−9]. Similar to the crystal diffraction for X-rays, TVBG can diffract the incident laser beam when its Bragg condition is satisfied. Based on the principle, the appropriate parameters of the grating can be selected to enable the low spatial frequency components of the incident beam to satisfy Bragg's law, while the high frequency components do not. Then, one-dimensional spatial filtering of a laser beam can be achieved without focusing[2]. Through proper configuration with another piece of grating, two-dimensional spatial filtering of the laser beam can be realized, as in the pin-hole spatial filter[3,4,9]. Although the pin-hole spatial filter is widely used for beam cleanup, its requisite focusing of the laser beam presents poor functionality, especially in high power laser fields. For example, because of the high power density vicinal to the pin-hole, the induced plasma may close the pin-hole, deflect the laser beam into the incident system, and probably damage the optical devices in the system. By contrast, TVBG can spatially filter the deformed laser beam directly without any focusing, avoiding the abovementioned drawbacks. Furthermore, TVBG filter occupies much less volume and weight than the pin-hole filter does. Thus, it can be used in air and space environments. With the advent of the novel recording material, photo-thermal-refractive (PTR) glass, which generates minimal loss in the visual, near, and middle infrared spectra[10], the application of TVBG in high power laser fields has been tremendously facilitated. Although TVBG theoretically has the potential to spatially filter the laser beam, few studies have presented an experimental analysis of its beam cleanup ability. Therefore, we design an experiment to verify its spatial filtering performance for spatially-deformed laser beams.

The configuration design of the experiment is depicted in Figure 1. In the diagram, f_0 denotes the period of the amplitude modulation plate, which is used to produce the spatially-deformed laser beam; D and D_{-1} denote the diameters of the He-Ne laser and the spatially-filtered beam, respectively; Λ and d represent the period and thickness of TVBG, respectively; θ_0 is the incidence angle of the central wave vector $\mathbf{k_0}$ of the deformed laser beam; K denotes the grating's vector, the module of which is $2\pi/\Lambda$. The beam profiler (BP) (BP109-UV, Thorlabs Corporation, USA) is used to detect the spatial electric field intensity distribution of the laser beam in the optical near field. The transmittance of the amplitude modulation plate is squarely modulated and can be

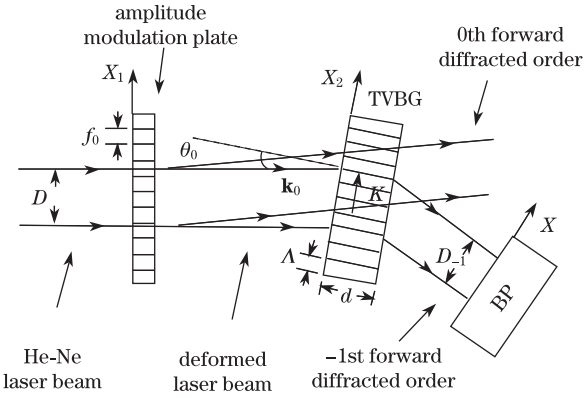

Fig. 1. Schematic of spatial filtering for deformed Gaussian laser beam by TVBG.

expressed as

$$T(x_1) = \begin{cases} 1, & mf_0^{-1} \le x_1 < (1/2+m)\, f_0^{-1} \\ 0, & (1/2+m)\, f_0^{-1} \le x_1 < (m+1)\, f_0^{-1} \end{cases}$$
$$m = 0, \pm 1, \pm 2, \cdots. \quad (1)$$

TVBG is recorded in PTR glass, fabricated by the Optigrate Corporation. It is used to spatially filter the deformed laser beam. It is a non-tilted sinusoidally-modulated grating, the refractive index of which is

$$n = n_0 + n_1 \sin(2\pi x_2/\Lambda), \quad (2)$$

where n_0 and n_1 denote the grating's mean refractive index and its modulation amplitude, respectively. The He-Ne laser operates at 632.8 nm, and its polarization is perpendicular to the plane of incidence. It is used to denote the undeformed laser beam. When the He-Ne laser propagates through the modulation plate, its spatial electric field amplitude is modulated, and the spatially-deformed laser beam is achieved. The intensity distributions of the He-Ne laser beam and the deformed laser beam after transmission through TVBG without any diffraction can be detected by the BP, as shown in Fig. 2.

In Figs. 2(a) and (b), both the horizontal axes denote lateral displacements, and vertical axes denote power. The total power levels of the He-Ne laser beam and the deformed laser beam are 7.9 and 4.2 mW, respectively, as recorded by the BP. The beam width D of the He-Ne laser beam is 1289 μm. Figure 2(b) shows that the intensity distribution of the deformed beam is amplitude-modulated and not smooth compared with that of the He-Ne laser beam. TVBG possesses excellent wave vector selectivity. Thus, we can enable the central wave vector $\mathbf{k_0}$ of the deformed beam satisfy the Bragg condition of TVBG. The intensity distribution of the -1st forward-diffracted order of the deformed beam by TVBG can also be detected by the BP, which is placed at the back surface of TVBG. Its intensity distribution recorded by the BP is shown in Fig. 3.

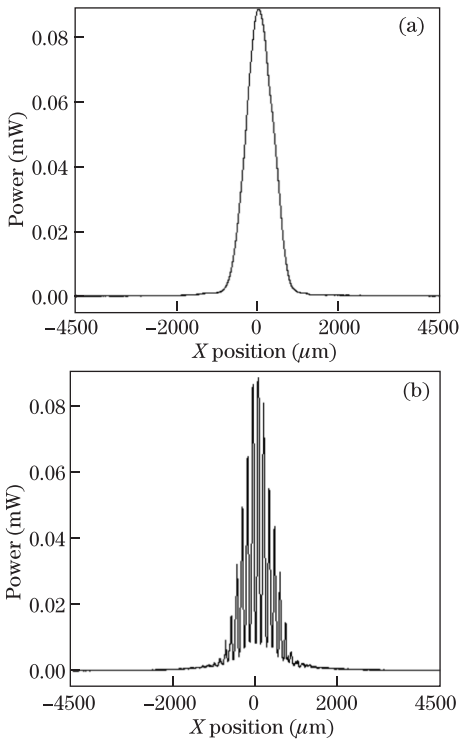

Fig. 2. Intensity distribution of (a) the He-Ne laser beam and (b) deformed laser beam transmitted through TVBG without any diffraction. $n_0 = 1.496$, $n_1 = 1.30 \times 10^{-4}$, $d = 3.06$ μm, $\Lambda = 2.88$ μm, and $f_0 = 7.2$ mm^{-1}.

In Fig. 3, the horizontal and vertical axes indicate the same denotations as those in Fig. 2. The intensity distribution of the -1st forward-diffracted order is smoothed compared with that in Fig. 2(b). Its beam width D_{-1} is 1395 μm, which is a little larger than that of the He-Ne laser. The beam width widening will be explained in the succeeding section. The intensity distribution of this order is similar to that of the He-Ne laser shown in Fig. 2(a), except for the total power differences between them. The total power of the -1st forward-diffracted order is 1.738 mW, as recorded by the BP.

Based on the rigorous coupled wave theory[11], we can theoretically analyze TVBG's spatial filtering for the deformed beam. Figure 4 shows the normalized spatial spectrum intensity distribution of the deformed beam and the diffraction efficiency of TVBG as a function of spatial frequency. From Fig. 4, we can determine that the deformed beam has a discrete spatial spectrum. The central component of the spatial spectrum (less than 1 mm^{-1}) exhibits information similar to

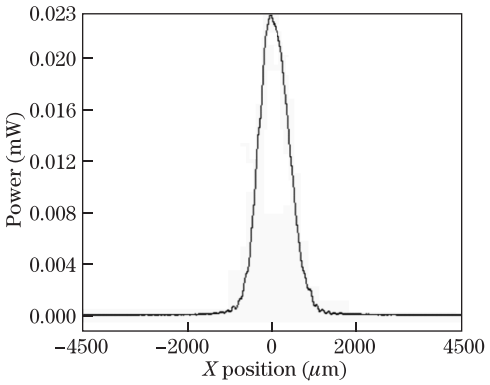

Fig. 3. Intensity distribution of the -1st forward-diffracted order.

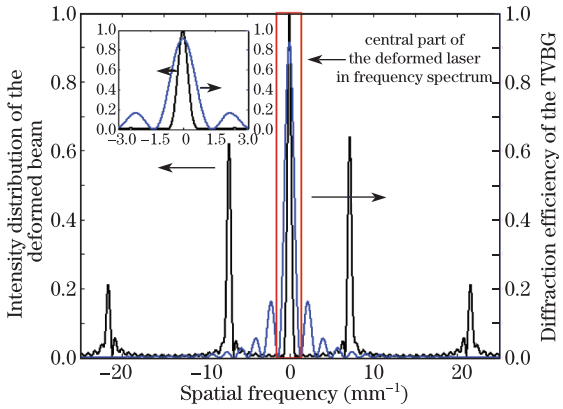

Fig. 4. Normalized spatial spectrum intensity distribution of the deformed beam and diffraction efficiency of TVBG as a function of spatial frequency.

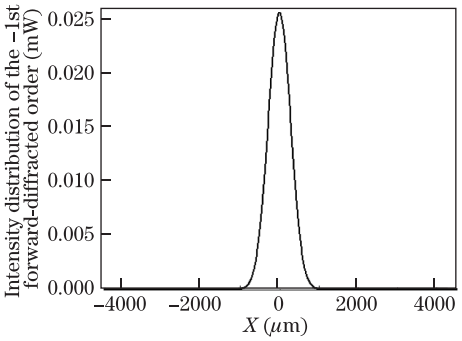

Fig. 5. Intensity distribution of the −1st forward-diffracted order by theoretical analysis.

the counterpart of the He-Ne laser, whereas the other components (more than 6 mm^{-1}) stand for the spatial noise caused by the modulation plate. TVBG has a spatial frequency selective bandwidth of less than 5 mm^{-1}. Thus, it can strongly diffract the central component (the calculated diffraction efficiency is up to 88.6%), while it minimally diffracts the components with higher spatial frequencies (the diffraction efficiency is nearly 0). The intensity distribution of the −1st forward-diffracted order is shown in Fig. 5.

Comparing Fig. 5 with Fig. 3, we observe that the intensity distribution of the −1st forward-diffracted order in the experiment is similar to that in the theoretical analysis, except for their minor power differences. Based on the modulation plate, the power of the central component is nearly half of the total power of the deformed laser beam, which is 4.2 mW as recorded by the BP. Therefore, the calculated power of the central component is 2.1 mW. The total diffraction efficiency of the central component of the deformed laser beam can be defined as

$$\eta = \frac{P_{-1}}{P_0}, \tag{3}$$

where P_0 and P_{-1} denote the power and its diffracted power of the central component of the deformed laser beam, respectively. With the experimental results, therefore, η is 82.9%. Based on the rigorous coupled wave theory, the calculated diffraction efficiency of the central component is up to 88.6%, which is larger than that generated in the experiment. The difference in total diffraction efficiency between them is caused by the reflection, minor absorption, and scattering of TVBG. The total diffraction efficiency can be improved by the antireflecting coating of TVBG.

The beam width widening between the He-Ne laser and the −1st forward-diffracted order is due to the diffractive characteristics of TVBG. Figure 4 shows that the central component of the spatial frequency spectrum of the deformed laser beam is not diffracted at the same diffraction efficiency. The diffraction efficiency of the higher spatial frequency components of the central part is less than that of the lower spatial frequency components. Thus, the beam width widens and is in good accordance with the theoretical analyses[12].

Figure 4 also shows that the side-lobes considerably influence the spatial frequency selective bandwidth of TVBG and limit its performance on spatial filtering with the lower spatial frequency modulation. However, several methods have been used to suppress side-lobes, such as using apodized TVBG[13].

In conclusion, we design an experiment in which the deformed laser beam is spatially filtered by TVBG. The deformed laser beam is produced by the He-Ne laser modulated by the amplitude plate with a spatial frequency of 7.2 mm^{-1}. The spatial profile of the −1st forward-diffracted order by TVBG is smooth and similar to that of the He-Ne laser. Furthermore, the experimental results are in good accordance with the theoretical results. The spatial filtering for the deformed laser beam can be achieved by TVBG at the near field. It is a potential substitute for the pin-hole filter, especially in high power laser fields.

This work was supported by the NSAF Foundation of the National Natural Science Foundation of China and the Chinese Academy of Engineering Physics (CAEP) under Grant No. 10676038. We also express appreciation for the TVBG provided by Optigrate Corporation.

References

1. A. Sevian, O. Andrusyak, I. Ciapurin, V. Smirnov, G. Venus, and L. Glebov, Opt. Lett. **33,** 384 (2008).
2. J. E. Ludman, J. R. Riccobono, N. O. Reinhand, I. V. Semenova, Y. L. Korzinin, S. M. Shahriar, H. J. Caulfield, J.-M. Fournier, and P. Hemmer, Opt. Eng. **36,** 1700 (1997).
3. G. Zheng, Y. He, S. Huang, J. Tan, X. Wang, and X. Wang, Acta Opt. Sin. (in Chinese) **29,** 863 (2009).
4. G. Zheng, J. Tan, Y. He, H. Zheng, X. Wang, and X. Wang, Acta Opt. Sin. (in Chinese) **30,** 1554 (2010)
5. C. Wang, L. Liu, A. Yan, D. Liu, D. Li, and W. Qu, J. Opt. Soc. Am. A **23,** 3191 (2006).
6. B. L. Volodin, S. V. Dolgy, E. D. Melnik, E. Downs, J. Shaw, and V. S. Ban, Opt. Lett. **29,** 1891 (2004).
7. G. B. Venus, A. Sevian, V. I. Smirnov, and L. B. Glebov, Opt. Lett. **31,** 1453 (2006).
8. A. Gourevitch, G. Venus, V. Smirnov, and L. Glebov, Opt. Lett. **32,** 2611 (2007).
9. M. Henrion, J. Ludman, G. Sobolev, S. Shahriar, S. Soboleva, and P. Hemmer, Proc. SPIE **3417,** 195 (1998).
10. L. Glebov, Proc. SPIE **6545,** 654507 (2007).
11. M. G. Moharam and T. K. Gaylord, J. Opt. Soc. Am. **73,** 1105 (1983)
12. G. Zheng, L. Li, Y. He, J. Tan, H. Zheng, X. Wang, and X. Wang, Acta Opt. Sin. (in Chinese) **29,** 126 (2009)
13. J. M. Tsui, C. Thompson, V. Mehta, J. M. Roth, V. I. Smirnov, and L. B. Glebov, Opt. Express **12,** 6642 (2004).